Technical Report No: ND09-2

RAPID AND SENSITIVE DETERMINATION OF BACTERIA IN WATER USING NANOPARTICLES

by

Yuhui Jin
Julia Xiaojun Zhao

Department of Chemistry
University of North Dakota, Grand Forks, North Dakota

November, 2009

North Dakota Water Resources Research Institute
North Dakota State University, Fargo, North Dakota

Technical Report No: ND09-2

RAPID AND SENSITIVE DETERMINATION OF BACTERIA IN WATER

USING NANOPARTICLES

By

Yuhui Jin[1]
Julia Xiaojun Zhao[2]
[1]WRRI Graduate Research Fellow and [2]Associate Professor
Department of Chemistry, University of North Dakota, Grand Forks, North Dakota

November 2009

Project Period: March 1, 2006 – February 28, 2009
Project Number: 2006ND98B, 2007ND151B, and 2008ND162B

North Dakota Water Resources Research Institute
North Dakota State University, Fargo, North Dakota

TABLE OF CONTENTS

LIST OF FIGURES

LIST OF SCHEMES

LIST OF TABLES

ACKNOWLEDGEMENTS

6

ABSTRACT

A series of new silica-based fluorescent nanoparticles were developed in this work. These nanoparticles can simultaneously emit fluorescence signals at different wavelengths. The principle of fluorescence resonance energy transfer (FRET) has been employed in making the fluorescent nanoparticles. The conditions for synthesis of the nanoparticles were optimized. These fluorescent nanoparticles have shown excellent photostability due to the protection of the silica nanomatrix. The surface of the multicolored fluorescent silica nanoparticles were functionalized using antibodies for recognizing pathogenic bacterial cells. Based on the antigen and antibody reaction, the nanoparticles were linked to the specific bacterial cells. Therefore, different types of bacterial cells were differentiated by the corresponding antibody-functionalized fluorescent silica nanoparticles.

INTRODUCTION

The determination of pathogenic bacteria is required in the fields of biotechnology, medical diagnosis, and water analysis.[1] However, Current methods using the conventional fluorophores are either time-consuming or insensitive. It is critical to develop a new method which can quickly identify pathogenic bacteria with high sensitivity. To achieve such a goal, fluorescent markers need to have intensified and stable fluorescence signals. In addition, multiple bacterial targets can be determined simultaneously by fluorescent markers. In this case, multiple fluorescent markers can be stimulated together by a single excitation source and generate different fluorescent colors.

Fluorescence nanomaterials are promising for biological target determinations because of their superior fluorescence properties to conventional fluorophores. For example, Quantum dots (QDs) are semiconductors with their sizes confined in several nanometers. Their fluorescence signals are intrinsically strong and highly resistant to photobleaching. In addition, their fluorescent spectra can be tuned by varying their sizes because of the quantum confinement effect.[2-5] Different colored QDs were used to label multiple samples simultaneously. Fluorescent silica nanoparticles have also been employed for fluorescence bioanalysis. Because these nanoparticles often encapsulate more than thousands of fluorophores in every individual nanomatrix, the fluorescence intensity of each nanoparticle can be thousands of times higher than the intensity of a single fluorophore. Trace amount of DNA and bacterial cells have been successfully identified and quantified by these highly-intensified fluorescence silica nanoparticles.[11] Another advantage of fluorescent silica nanoparticles is their biocompatibility. Composed of amorphous silica, these nanoparticles possess much less toxicities compared to the heavy-metal-contained QDs.[6-10, 12] In this sense, fluorescent silica nanoparticles are

8

considered more suitable in the *in vitro* and *in vivo* bioanalyses, which generally require nontoxic markers in measurement.

Fluorescent silica nanoparticles need to be encoded with different colors for detecting multiple biological targets, such as different types of bacteria. These fluorescent silica nanoparticles should be sufficiently stimulated together and express different fluorescent colors. To attain this property, nanoparticles need to dope multiple fluorophores in the silica matrices, and different types of fluorophores should be spatially close to each other for an efficient fluorescence resonance energy transfer (FRET). Because it is difficult to conjugate different fluorophores together by the current strategies, synthesizing multicolor-encoded fluorescent silica nanoparticles is still challenging. Strategies of fluorophore conjugation and the synthesis of multicolor-encoded silica nanoparticles are vital for an efficient and sensitive bacterial determination.

In this work, an avidin-biotin bridge was employed to conjugate fluorophores together and to precisely control the distance between them. Basically, fluorophores are initially conjugated to avidin and biotin groups and then closely link together through the highly specific and stable avidin-biotin binding. The conjugates which formed in this way exhibited a highly efficient FRET. As a result, different conjugates can be excited simultaneously and generate different fluorescent colors. In addition, the performance of the conjugates can be further improved by encapsulating them in silica matrices. Here, the reverse microemulsion method was conducted for doping the water-soluble conjugates into silica nanoparticles. The conjugates can be permanently trapped in the negatively charged silica nanomatrix because of their high molecular weight and positive charges. These multicolor-encoded nanoparticles exhibit several advantages over

traditional fluorophores. First, these nanoparticles have strong and stable fluorescent signals which are highly resistant to photobleaching. Second, these multicolor fluorescent silica nanoparticles exhibit a great potential for identifying and quantifying multiple biological targets simultaneously. Finally, the surfaces of these silica nanoparticles are easily modified with various types of functionalized groups, such as antibodies and protein molecules. In this study, three pathogenic bacterial cells, Klebsiella pneumoniae (KP), Pseudomonas aeruginosa (PA), and Staphylococcus aureus (SA) were simultaneously identified by the corresponding antibody-functionalized silica nanoparticles, which contain different fluorescent colors.

METHOD

Materials

Biocytin-Oregon Green 488, biotin-dextran-TMR and avidin-Texas Red were purchased from Molecular probes. 99.999% tetraethoxylorthosilicane (TEOS), EDC and NHS were from Aldrich. N-(trimethoxysilylpropyl)-ethylenediamine,triacetic acid trisodium salt 45% in water was purchased from Gelest Inc. Three types of bacterial cells (*klebsiella pneumoniae* (KP), *pseudomonas aeruginosa* (PA), *staphylococcus aureus* (SA)) were obtained from American Tissue Culture Collection (ATCC). Antibody against PA was from Dr. Gerald Pier (Harvard Medical School). Antibody against KP was purchased from Biogenesis. SA antibody (Mouse IgM ascites) was from Santa Cruz Biotechnology. Phosphate buffer (PB, 10 mM, pH 7.0) and 2-morpholinoethanesulfonic acid (MES) buffer (0.1 M, pH 6.0) were used during the cell imaging and bioconjugation.

Conjugation of Fluorophore Molecules for FRET

The conjugation was based on a reaction between biocytin and avidin. Fluorophores with biocytin group, biocytin-oregon green 488 (BOG), biotin labeled dextran-TMR (DTB) can conjugate with the avidin conjugated fluorophores, avidin conjugated texas red (ATR) and avidin conjugated fluorescein (AFC). The stock solutions of the fluorophores were first prepared by dissolving fluorophores in a 10 mM PBS buffer (pH = 7.4). The prepared stock solutions contain 1 mM of avidin or biocytin. In the second step, the fluorophore conjugates were directly mixed together. After a short vortexing, the mixture was kept in darkness for 15 mins. Because each avidin molecule can react with up to 4 biocytin units, the ratio of fluorophores is able to be adjusted. For example, in the 3-fluorophore conjugate experiment, the fluorophore ratio were manipulated by simply changing the ratio of the stock solutions added (Table 1). In the control experiment, DTMR, which does not conjugate to biocytin or avidin, was employed. Basically, DTMR and AFC were mixed together following the same procedure for the preparation of fluorophore-conjugates.

Synthesis of FRET-based Fluorescent Nanoparticles

The FRET-based fluorescent silica nanoparticles were synthesized by doping the FRET-based conjugates into a silica matrix using a reverse microemusionmethod.[11, 13-16] Briefly, a water-in-oil microemulsion was prepared by mixing 1.77 mL of Triton X-100, 1.8 mL of *n*-hexanol, 7.5 mL of cyclohexane, and 480 μL of dye mixture containing 120 μL of dye conjugate solution and 360 μL of water. A silica precursor (80 μL of TEOS) was added to the microemulsion followed by 20 min of stirring. Hydrolysis and polymerization of TEOS was initiated by 60 μL of NH_4OH. The reaction was allowed to

continue for 24 h stirring at room temperature. Finally, a FRET-based fluorescent silica nanoparticle was produced.

In order to immobilize antibodies on the nanoparticle surface, it is essential to have carboxyl groups on the nanoparticles. The carboxyl-modified surface was obtained by a post-coating step in the synthesis. A 20 μL aliquot of TEOS and 20 μL of N-(trimethoxysilylpropyl)-ethylenediamine, triacetic acid trisodium salt (45 % in water) was added to the microemulsion for a continuous polymerization of 24 h under magnetic stirring. Then, the microemulsion was broken by an addition of 20 mL of acetone to the microemulsion. To harvest the nanoparticles, sonication, vortex, and centrifugation were employed. Finally, the resultant nanoparticles were washed three times with a 95 % ethanol and water.

Characterization of Fluorescence Properties

The fluorescence properties of fluorophores, the fluorophore conjugates and the multicolor-encoded nanoparticles were characterized by a Jobin Yvon Horiba Fluorolog spectrofluorometer. To prevent self-quenching, fluorophores and fluorescent nanoparticles need to be diluted to a proper concentration for measurements. For example, fluorophores and fluorophore conjugates were first diluted from the stock solution to 10 nM by a 10 mM PB. The nanoparticles were dissolved in a 10 mM PB with a final concentration of 0.1 mg/mL. The pH of all the solutions was buffered by PB at 7.4 to provide a stable and repeatable fluorescent result. The excitation wavelength of all the experiments was set at 488 nm for the fair comparison of the efficiency of FRET among fluorophores and multicolor-encoded nanoparticles.

Surface Immobilization of Antibody Molecules onto the Nanoparticles.

The immobilization of antibody molecules onto nanoparticles was conducted according to the literature method.[17] Briefly, 0.2 mg of nanoparticles was dissolved in a 100 µL of 0.1 M MES buffer (pH =6.0). Then 500 µL of 4 mM EDC and 10 mM sulfo-NHS were prepared in the MES buffer. The two solutions were mixed with a continuous stirring of 15 min. In this process, the carboxyl groups on the nanoparticle surface were activated. The EDC-activated nanoparticles were then separated from the solution by centrifuging at 11.0 k rpm for 10 min. Then, the EDC-activated nanoparticles were resuspended into a 0.1 M PB buffer (pH =7.4) to form a 0.1 mg/mL solution which was ready for conjugation of antibodies. An aliquot of 20 µg of antibody (1mg/mL in PBS) was added to the nanoparticle solution. After 2 h gently shaking, the conjugated nanoparticles were centrifuged and washed with the PB buffer. The nanoparticles were then resuspended into a 1 mL of PB buffer. Un-reacted carboxyl groups on the nanoparticle surface will be blocked by 0.05 % BSA 0.5 h. Finally, the antibody-immobilized nanoparticles were collected by centrifuging and stored in a 200 µL of PB buffer at 4 ℃.

Detection of Bacteria Cells using the Nanoparticles.

The fluorescence determination of bacterial cells by multicolor-encoded nanoparticles was monitored by a Carl Zeiss LSM 510 Meta laser scanning confocal microscope. In the first step, bacterial sample was prepared. About 10^7 fresh harvested bacterial cells were centrifuged down at 2000 rpm for 10 min. Then, the pellet was washed by PBS, and resuspended in 100 µL PBS solution (pH 7.4). Second, the purified bacterial cells were relocated to a glass bottom culture plate from which bacteria can be

directly monitored using the confocal fluorescence microscope. Both the fluorescence and blackfield images were taken as controls. Then, a 100 μL aliquot of antibody coated nanoparticles were added into the culture plate (nanoparticles: bacteria = 10000:1). After a gentle mixing, the mixture was incubated at 37 ℃ for 5 min. Finally, the fluorescence images of the FRET nanoparticle labeled bacteria were characterized using the confocal fluorescence microscope. The multiple bacteria measurements were followed a similar procedure. Expect, different types of bacteria were purified and located to the glass plate together, and different antibody modified nanoparticles were added to the bacterial solution simultaneously. All the confocal fluorescence measurements of bacteria were carried out at 37 ℃.

RESULTS AND DISCUSSION

Fluorescence Properties of Fluorophore Conjugates

One basic requirement for FRET is that the spatial distance between donor and acceptor fluorophores must be small (less than 10 nm). In this study, fluorophores were brought together in a short distance through an avidin-biotin binding. The binding here is crucial for the FRET among the conjugated fluorophores. It keeps the fluorophores in close proximity for an efficient FRET. In fact, the FRET is unlikely to occur without the assistance of the avidin-biotin linkage. In addition, the FRET efficiency of the conjugates is highly reproducible, since the reaction between avidin and biotin is highly specific and always brings the conjugated fluorophores together in the same manner. Because the binding between avidin and biotin is spontaneous and highly favorable, fluorophores with biotin and avidin groups are assumed to conjugate together in fifteen minutes by simply mixing them in a phosphate buffer (pH = 7.4). In a dual-fluorophore system, fluorescein

and TMR serve as the donor and accepter fluorophores, respectively. When the mixture of donor and accepter is excited by a single excitation light at 488 nm, the accepter fluorophore cannot be sufficiently stimulated unless it receives the energy from an excited donor in close proximity. For example, the biotin conjugated dextran-TMR (DTB) showed a 22% increase in fluorescence intensity after binding to the avidin conjugated fluorescein (AFC) (Figure 1, B). Without the avidin-biotin linkage, in comparison, no FRET phenomenon was observed between AFC and detran-TMR (DTMR, no biotin) (Figure 1, A).
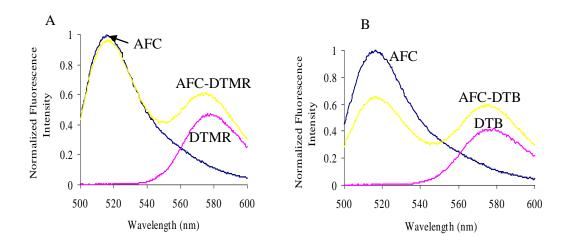

Figure 1. FRET between AFC and DTB. (A) Fluorescence spectra of AFC, DTB and AFC-DTB conjugates; (B) Control experiment, AFC, Dextran-TMR (DTMR) and the mixture of AFC and DTMR.

The avidin-biotin bridge is also capable of mediating a triple-fluorophore FRET. Because every avidin molecule can bind up to four biotin molecules, multiple types of fluorophores can first conjugate to avidin and biotin molecules, respectively, and then link together through the avidin-biotin binding. Here, Oregon Green 488, TMR and Texas red were employed for a triple-fluorophore FRET study because of the sufficient overlap of their emission and excitation spectra (Figure 2). In addition, these fluorophores

were spontaneously conjugated together after being linked to avidin or biotin moieties. For instance, biotinylated Oregon Green 488 (BOG), biotinylated detran-TMR (DTB), and avidin-functionalized Texas Red (ATR) were conjugated at various ratios (Table 1) by simply blending these fluorophores in a phosphate buffer (10 mM, pH = 7.4).
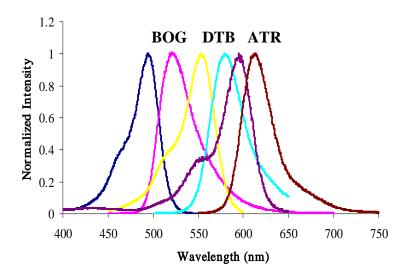

Figure 2. Normalized excitation and emission spectra of BOG, DTB and ATR.

In all the multi-fluorophore conjugates, a BOG moiety served as the FRET donor to transfer energy to the acceptor fluorophores, DTB and ATR. FRET phenomena have been observed in both the dual-fluorophore conjugates (DTB-ATR conjugates, mole ratio of DTB: ATR = 2: 3, Figure 10, A) as well as in the triple-fluorophore conjugates (BOG-DTR-ATR conjugates, mole ratio of BOG: DTR: ATR = 2:2:3, Figure 3, B). For instance, in the case of DTB-ATR conjugates, the donor fluorophore DTB lost nearly 40% of its fluorescence intensity; while the acceptor, ATR, showed a 150% increase in the fluorescence at the same time (Figure 3, A). In triple-fluorophore conjugates, the energy of the excited donor (BOG) transferred to the ultimate acceptor ATR directly, or was indirectly mediated by DTB. The direct energy transfer between BOG and ATR is

possible; however, the efficiency of FRET is low because of the insufficient overlap of their emission and excitation spectra (Figure 2). Therefore, the indirect FRET pathway is vital for an efficient FRET between BOG and ATR. In this case, DTB first received the energy from the donor molecule, BOG. After that, the stimulated DTB might further deliver the energy to the terminated acceptor ATR. As a result, the fluorescence intensity of ATR was enhanced more than 9 times (Figure 3, B).
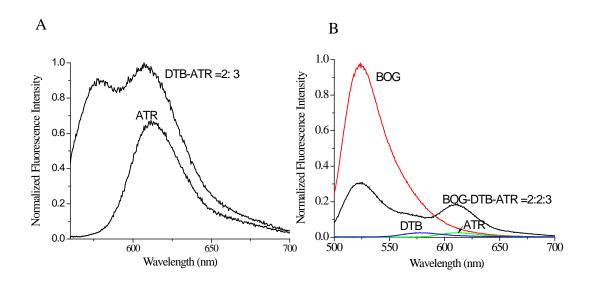

Figure 3. FRET of fluorophore-conjugates via avidin-biotin bridge. (A) Fluorescence spectra of ATR and DTB-ATR conjugates; (B) Fluorescence spectra of BOG, DTB, ATR and the triple-fluorophore conjugates.

Table 1. Ratio of fluorophores for conjugation through the avidin-biotin bridge.

No.	BOG (μL)	DTB (μL)	ATR (μL)	Avidin (μL)	Fluorophore Ratio: (BOG: DTB: ATR)
1	40	-	-	30	4: 0: 0
2	5	35	-	30	0.5: 3.5: 0
3	-	40	-	30	0: 4: 0
4	5	30	30	-	0.5: 3: 3
5	5	-	30	-	0.5: 0: 3
6	-	-	30	-	0: 0: 3

Based on current investigation of these fluorophore conjugates, avidin-biotin linkage is able to integrate multiple fluorophores in close proximity. The procedure is spontaneous and simple with high reproducibility. Through the avidin-biotin bridge, fluorophores were tightly bonded together and could easily pass the fluorescence energy from one to another. By adjusting the type and ratio of fluorophores in the avidin-biotin conjugation (Table 1), the excitation and emission spectra of the newly formed conjugates are tunable. These fluorophore-conjugates are good fluorescent probes and can be potentially used in multiple-biological-target determinations.
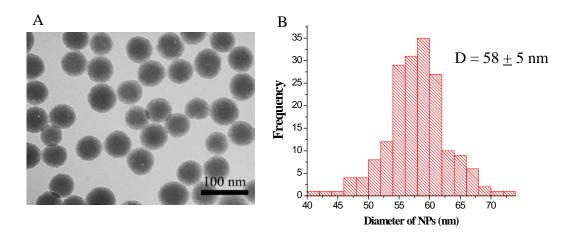

Figure 4. Size distribution of BOG-DTB conjugate doped nanoparticles. (A) TEM image of multicolor-encoded nanoparticles; (B) Histogram of the diameter of the nanoparticles measured from TEM images (More than 75 nanoparticles were measured).
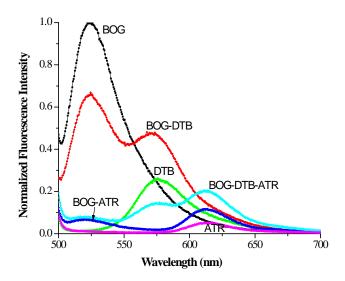
Figure 5. Fluorescence spectra of fluorophore-conjugated nanoparticles.

Fluorophore-conjugate Doped Silica nanoparticles

The fluorescent probes produced using avidin-biotin bridges are promising in bioanalysis because of their tunable excitation and emission spectra. However, these probes are still vulnerable to photobleaching and suffer from the low fluorescence intensity, both of which greatly limit their applications in current bioanalyses. To deal with these challenges, the avidin-biotin associated conjugates were doped inside silica matrix using a reverse microemulsion approach. Because numerous hydrophilic conjugates can be trapped in a single silica nanoparticle; the fluorescence intensity of one conjugate-doped nanoparticle is much higher than a single conjugate. In addition, the fluorescence of the conjugates can be protected from fluorescence quenchers by the silica matrix. Compared to the pure conjugates, the conjugate-doped nanoparticles are easily functionalized for the specific target-determination.

Figure 6. Fluorophore-conjugate doped nanoparticles illuminated under 365 nm UV light (From left to right are nanoparticles doped with conjugates from 1 to 6 listed in Table 1).

In this study, multiple-fluorophore conjugates were encapsulated in silica nanoparticles using the reverse microemulsion method. In a typical synthesis, the nanoparticles have a uniform size with a diameter of 58 ± 5 nm confirmed by their TEM image (Figure 4). The surfaces of the nanoparticles have been modified with carboxyl groups for further conjugation to antibody or other target-directing molecules. These nanoparticles also exhibited good solubility in biological conditions with no apparent aggregation observed in the aqueous solution (Figure 4, A).

The fluorescence properties of the conjugates, including the FRET patterns, can be easily tuned in the conjugation step, and well-preserved throughout the process of nanoparticle synthesis. Suspended in the water droplet of the reverse microemulsion, the configuration and properties of the conjugates were not disrupted. Even after the entrapment, the fluorescence properties of the conjugates were well-kept. The fluorescence spectra of the conjugate-doped nanoparticles revealed that the FRET

20

processes were preserved and that the probes could be used for multiple-target determination (Figure 5). All of these nanoparticles can be efficiently stimulated and exert different fluorescence signals by a single excitation source at 488 nm (Figure 5). This result has been also proved by exposure to the phosphate-buffer-suspended nanoparticle solutions under with a UV light at 365 nm. All of the solutions generated strong fluorescent colors with the stimulation (Figure 6).

In addition, the conjugate-doped silica nanoparticles showed superior photostability to that of the free conjugates. In a model experiment, for example, under the irradiation of a 450 W xenon lamp for 0.5 h, the fluorescence intensity of the rhodamine-6G (which has similar structure and properties to DTMR) decreased to 34%, while the DTMR doped nanoparticles showed a fairly stable fluorescence signal (more than 90% of the fluorescence signal was reserved) (Figure 7). The higher photostability of the conjugate-doped nanoparticles is attributed to the protection from the silica matrix. The silica matrix can extensively slow down the diffusion of quencher molecules or even prohibit the direct contact between quenchers and fluorophores. In consequence, the fluorescence of the doped fluorophores and conjugates were much more stable. Both the tunable fluorescence spectra and the highly stabilized fluorescence signals suggest that the conjugate-doped nanoparticles are favorable for long-term, multiple-target bioanalysis.
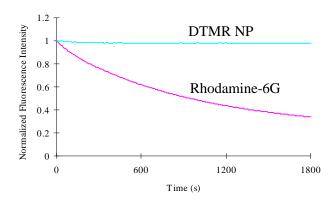
Figure 7. Photostabilities of Rhodamine 6G and DTMR doped nanoparticles.

Simultaneously detection of different types of bacteria cells by multicolor-encoded nanoparticles

In this approach, various multicolor-encoded nanoparticles were functionalized with different antibodies for the detections of PA, KP and SA bacteria, respectively. Thus, different bacteria could be labeled by these nanoparticles and differentiated from the color of the nanoparticles. Remarkably, these antibody-functionalized nanoparticles were able to identify the specific bacteria in 5 min. For example, SA bacteria exhibited strong fluorescence signals after the addition of antibody-functionalized nanoparticles in 5 min (Figure 8). The quick response of the detection can be attributed to the intensified fluorescence of the nanoparticles. Even each bacterium was only labeled by a few of nanoparticles in a short time, the intensity of these fluorescent nanoparticles were high enough to visualize the bacterium under a fluorescence microscope. In addition, each nanoparticle was able to integrate several antibodies on its surface. By combining the

22

power of multiple antibodies onto an individual nanoparticle, the nanoparticle might recognize targets more rapidly and accurately.

The antibody-functionalized silica nanoparticles also showed a good selectivity in bioanalysis. Because the nanoparticles were modified by antibodies, the antibodies were able to direct the nanoparticles to the target-bacteria. Other bacteria, however, cannot be efficiently labeled by these nanoparticles because of lacking of specific binding. For example, SA bacteria were labeled by the corresponding antibody-functionalized nanoparticles in the presence of another type of bacteria, PA. In 5 min, the SA bacteria were successfully marked by the nanoparticles, while the PA bacteria showed with no fluorescent color (Figure 9).

Finally, three types of bacteria (PA, KP and SA) and those antibody-functionalized multicolor-encoded silica nanoparticles were mixed together in one pot. Again, in 5 min, bacteria were specifically labeled with the corresponding antibody-functionalized nanoparticles. Under a confocal fluorescence microscope, these bacteria were differentiated by the fluorescent color of the nanoparticles that attached on them (Figure 10). This experiment clearly showed the feasibility and practicality of the multicolor-encoded fluorescent silica nanoparticles in a simultaneous multiple-biological-target determination.
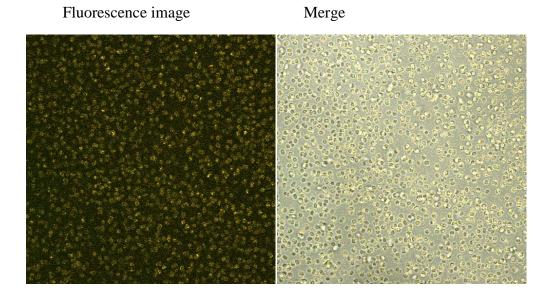
Figure 8. Fluorescence images of SA bacteria cells labeled by SA antibody linked BOG-ATR dye doped nanoparticles. The color showed in the fluorescence image is pseudo-color.
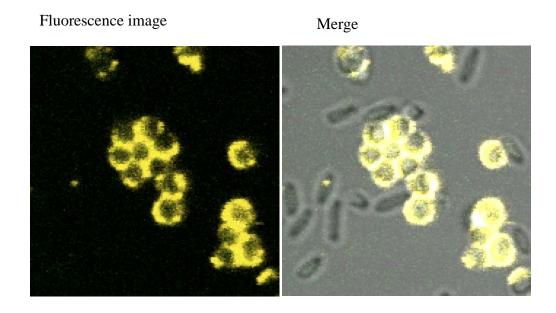
Fluorescence image   Merge

Figure 9. Fluorescence images of SA and PA bacteria cells after being labeled with SA antibody- linked BOG-ATR dye-doped nanoparticles. PA bacteria were employed as control cells, and showed no change before and after the addition of nanoparticle solution, while SA bacteria cells were marked by nanoparticles after 5 min of incubation.
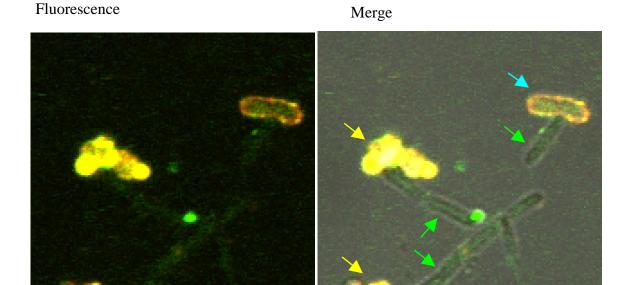
Figure 10. Simultaneously detection of SA, PA and KP bacteria using correspoinding antibody linked multicolor-encoded nanoparticles. The light blue arrow points to the location of KP bacterium, the yellow arrows point to the location of SA bacteria, and the green arrows point to the location of PA bacteria.

CONCLUSIONS

So far, a series of multicolor-encoded nanoparticles have been successfully developed for simultaneous determination of multiple bacterial targets. By a reverse microemulsion method, these multicolor-encoded nanoparticles were easily to be modified with different functional groups. Their sizes were highly uniformed and distributed in a relatively narrow range. The outstanding fluorescence properties, such as versatile fluorescence spectra, strong and stable fluorescence signal, have been achieved by doping the avidin-biocytin/biotin dye conjugates into the silica shell. Because different dye molecules are closely conjugated through the avidin-biocytin bridge, the fluorescence energy has been transferred from one to another. Then different dye conjugates can be illuminated as the same time by a single excitation source. These basic spectral properties of the dye conjugates have been well conserved after being doped inside nanoparticles, as the same time, the photostabilities were dramatically enhanced due to the protection of

silica shell. After being linked with antibody, the multicolor-encoded nanoparticles were employed to probe bacteria cells. Under a confocal fluorescence microscope, different types of bacteria, SA, PA and KP, have been successfully labeled by multicolor-encoded nanoparticles. In the control experiment, only SA bacteria were labeled by the SA-antibody coated nanoparticles, no PA bacteria were marked by these nanoparticles. This suggest our antibody linked nanoparticles have a great selectivity. In the future, our work will focus on the simultaneously detection of different bacteria samples with high selectivity.

REFERENCES

(1)   Zhao, X.; Hilliard, L. R.; Wang, K.; Tan, W., Bioconjugated Silica Nanoparticles for Bioanalysis. In Encyclopedia of Nanoscience and Nanotechnology, Nalwa, H. S., Ed. American Scientific Publishers: Stevenson Ranch, 2004; pp 255-268.

(2)   Akerman, M. E.; Chan, W. C.; Laakkonen, P.; Bhatia, S. N.; Ruoslahti, E. *Proc. Natl. Acad. Sci. U S A* 2002, *99*, 12617-12621.

(3)   Bakalova, R.; Zhelev, Z.; Aoki, I.; Ohba, H.; Imai, Y.; Kanno, I. *Anal. Chem.* 2006, *78*, 5925-5932.

(4)   Bruchez, M. J.; Moronne, M.; Gin, P.; Weiss, S.; Alivisatos, A. P. *Science* 1998, *281*, 2013-2016.

(5)   Yang, L.; Li, Y. *Analyst* 2006, *131*, 394-401.

(6)   Derfus, A. M.; Chan, W. C. W.; Bhatia, S. N. *Nano Lett.* 2004, *4*, 11-18.

(7)   Hoshino, A.; Fujioka, K.; Oku, T.; Suga, M.; Sasaki, Y. F.; Ohta, T.; Yasuhara, M.; Suzuki, K.; Yamamoto, K. *Nano Lett.* 2004, *4*, 2163-2169.

(8)   Kirchner, C.; Liedl, T.; Kudera, S.; Pellegrino, T.; Javier, A. M.; Gaub, H. E.; Stoelzle, S.; Fertig, N.; Parak, W. J. *Nano Lett.* 2005, *5*, 331-338.

(9)   Lovrić, J.; Bazzi, H. S.; Cuie, Y.; Fortin, G. R. A.; Winnik, F. M.; Maysinger, D. *J. Mol. Med.* 2005, *83*, 377-385.

(10) Shiohara, A.; Hoshino, A.; Hanaki, K.; Suzuki, K.; Yamamoto, K. *Microbiol. Immunol.* 2004, *48*, 669-675.

(11) Zhao, X.; Tapec-Dytioco, R.; Tan, W. *J. Am. Chem. Soc.* 2003, *125*, 11474-11475.

(12). Jin, Y.; Kannan, S.; Wu, M.; Zhao, X. *Chem. Res. Toxicol.* 2007, ASAP

(13) Santra, S.; Wang, K.; Tapec, R.; Tan, W. *J. Biomed. Opt.* 2001, *6*, 160-166.

(14) Santra, S.; Zhang, P.; Wang, K.; Tapec, R.; Tan, W. *Anal. Chem.* 2001, *73*, 4988-4993.

(15) Zhao, X.; Bagwe, R. P.; Tan, W. *Adv. Mater.* 2004, *16*, 173-176.

(16) Zhao, X.; Hilliard, L. R.; Mechery, S. J.; Wang, Y.; Bagwe, R. P.; Jin, S.; Tan, W. *Proc. Natl. Acad. Sci. U.S.A.* 2004, *101*, 15027-15032.

(17) Wang, L.; Zhao, W.; O'Donoghue, M. B.; Tan, W. *Bioconjug. Chem.* 2007, *18*, 297-301.